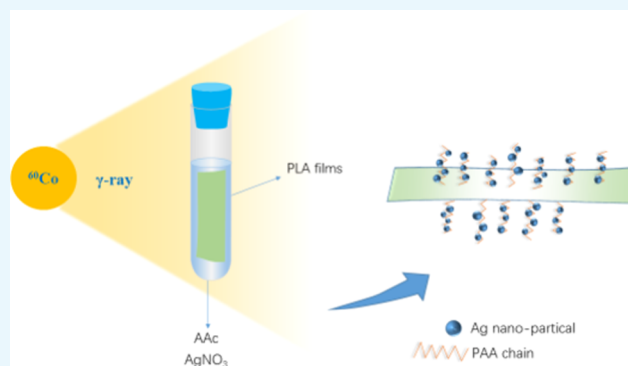


# Hydrophilic and Antibacterial Modification of Poly(lactic acid) Films by $\gamma$ -ray Irradiation

Yue Qi, Hui-Ling Ma, Zhong-He Du, Bo Yang, Jing Wu, Rui Wang,<sup>✉</sup> and Xiu-Qin Zhang\*<sup>✉</sup>

Beijing Key Laboratory of Clothing Materials R & D and Assessment, Beijing Engineering Research Center of Textile Nanofiber, School of Materials Design & Engineering, Beijing Institute of Fashion Technology, Beijing 100029, China

**ABSTRACT:** To improve the hydrophilicity and imparting antibacterial properties to poly(lactic acid), poly(acrylic acid) (PAA) and silver particles (AgNPs) were simultaneously introduced onto the surface of poly(lactic acid) (PLA) films by  $\gamma$ -ray irradiation. The morphology and structure of the modified films were characterized by scanning electron microscopy (SEM)/energy-dispersive X-ray (EDX) spectrometry and Fourier transform infrared (FTIR) spectroscopy. The interaction between PAA and AgNPs was investigated by X-ray photoelectron spectroscopy (XPS), confirming the coordination between AgNPs and the oxygen atom on the carboxylic group of PAA. The contact-angle (CA) measurements and antibacterial tests showed that the modified PLA films with a low silver content (PLA-g-PAA-Ag) exhibited excellent hydrophilicity as well as antibacterial activity compared with the neat PLA film.



## 1. INTRODUCTION

Poly(lactic acid) (PLA) is an environmentally friendly polymer with promising applications due to its renewability, biodegradability,<sup>1</sup> biocompatibility,<sup>2</sup> excellent thermomechanical properties,<sup>3,4</sup> and good processing properties.<sup>5</sup> It has been applied in the biomedical field such as in absorbable surgical sutures,<sup>6</sup> skeleton materials,<sup>7</sup> disposable isolation pads, and drug delivery systems,<sup>8–10</sup> as well as clothing fabrics and textiles.<sup>11</sup>

As a polyester, PLA has poor hydrophilicity and low functionalization capacity,<sup>12</sup> which seriously affect its application in clothing, medical supplies, and other fields. Various physical and chemical methods have been applied to improve the hydrophilicity of PLA. Blending is one of the simplest methods by combining different components with different properties. The hydrophilic polymers such as starch,<sup>13</sup> citrate plasticizer, and other hydrophilic substances were blended with PLA,<sup>14</sup> and the hydrophilicity as well as mechanical properties of the blends can be regulated by adjusting the blending ratio. In addition, the morphologies of fibers' cross-sections also play an important role in hydrophilicity. Taking advantages of larger voids and surface area provided by the profiled cross-section, fibers with hetero-morphologies exhibit better hydrophilicity and moisture permeability than those fibers with round-shaped cross-sections.<sup>15</sup> What is more, some functional groups can also be introduced onto PLA fibers by chemical reactions to improve its hydrophilicity.<sup>16</sup> Among these methods, the chemical methods of introducing hydrophilic groups is an efficient way because the PLA can be modified at the molecular level.<sup>17,18</sup> For example, PLA and poly(ethylene glycol) (PEG) containing hydrophilic segments were chemically copolymerized to prepare PLA-*b*-PEG-*b*-PLA tri-block copolymers with

different PEG contents.<sup>19</sup> The water contact angle of the copolymers decreased from 79.0 to 33.5° with increasing PEG contents. The obtained block copolymers can potentially be used to prepare controlled drug release microcapsules. Other reagents with hydrophilic groups, such as N-vinylpyrrolidone (NVP) and acrylic acid can also be applied to improve the hydrophilicity of PLA by ring-opening grafting or melt condensation with PLA.<sup>20,21</sup>

Moreover, the antibacterial activity of PLA is also one of the foremost considerations in some fields, especially fabrics. Antibacterial agents, such as nanosilver,<sup>22,23</sup> allyl isothiocyanate,<sup>24</sup> or chitin,<sup>25</sup> were introduced into PLA. Mao et al.<sup>26</sup> prepared a double antibacterial coating (PPy/Ag) by polymerizing pyrrole (Py) on the surface of a PLA film. Silver ions (Ag<sup>+</sup>) were used to initiate the oxidation of pyrrole and render antibacterial properties to the obtained coating. The total number of *Escherichia coli* colonies of the modified PLA film was reduced by more than four orders of magnitude compared with that of the pure PLA film. Fei et al.<sup>27</sup> synthesized PLA/tea polyphenol nanofibers with great antibacterial activity. The inhibition rates of nanofibers on *E. coli* and *S. aureus* were 96.9 and 97.6%, respectively.

$\gamma$ -Ray irradiation has been widely used in the modification of PLA due to its simple and controllable reaction conditions, low energy consumption, and environmental friendliness.<sup>28,29</sup> It has been reported that poly(ethylene-co-vinyl alcohol) (EVOH) and PLA blends were modified in the presence of

Received: September 23, 2019

Accepted: November 15, 2019

Published: December 4, 2019

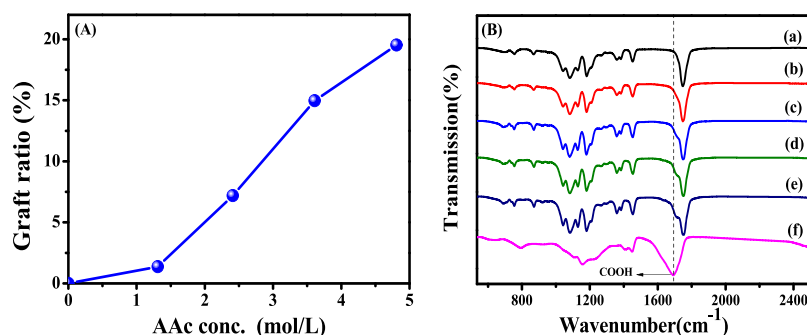


**Figure 1.** (A) Effect of monomer concentration on the GY at a dose rate of 50 Gy/min and a total dose of 10 kGy (B) FTIR spectra of PLA, PLA-g-PAA, and PAA (a, PLA; b–e, PLA-g-PAA-1–4; f, PAA).

triallyl isocyanurate (TAIC) by  $\gamma$ -ray irradiation.<sup>30</sup> The heat distortion temperature of the irradiated blends has dramatically increased from 70 °C (neat PLA) to 140 °C. Chen et al.<sup>31</sup> reported that NVP was grafted on PLA under  $\gamma$ -ray irradiation. The water contact angle of the modified PLA film decreased with the increase of the grafting yield of poly(vinyl pyrrolidones) (PVP). When the grafting yield was 41.3 wt %, the contact angle decreased from 75.1 to 50.3°. Therefore, high-energy irradiation is an effective way to modify PLA.

In this work, PLA films were endowed with hydrophilicity and antimicrobial properties by  $\gamma$ -ray irradiation. A hydrophilic monomer, acrylic acid (AAc), was modified on the surface of PLA films by the  $\gamma$ -ray-induced grafting polymerization. The effect of monomer concentration on the grafting yield and hydrophilicity was systematically studied. The silver nanoparticles (AgNPs) were further loaded on the surface of PLA by  $\gamma$ -ray-induced reduction to improve the antibacterial activity of PLA. The antibacterial rate of the grafted film with AgNPs to *E. coli* and *S. aureus* was more than 99%, and the water contact angle decreased from 94.5 (neat PLA film) to 64.1°.

## 2. RESULTS AND DISCUSSION

### 2.1. Structure Analysis of Radiation-modified PLA.

**2.1.1. Characterization of PLA-g-PAA Films.** The effect of the monomer concentration of acrylic acid on graft yield (GY) is shown in Figure 1A. It is shown that the GY increases with the increase of monomer concentration. The concentration of the diffused monomer in the PLLA matrix increases with the increased monomer concentration in the solution, which is facilitated by AAc grafting. When the monomer concentration is 4.82 mol L<sup>-1</sup>, the GY reaches 19.53 wt %. A further increase of the AAc concentration leads to self-polymerization of the AAc monomer. The homopolymerization of AAc is not beneficial to monomer diffusion and grafting because of the increased viscosity.<sup>32</sup>

FTIR spectra of PLA, PLA-g-PAA, and PAA homopolymer gels are presented in Figure 1B. A strong band at 1748 cm<sup>-1</sup> can be found in all of the PLA samples, which can be assigned to the C=O stretching vibration of PLA.<sup>33</sup> Since this group does not change in the reaction, the curves of PLA and PLA-g-PAA were normalized based on this band. For PLA films, there are two characteristic bands at 1435 and 748 cm<sup>-1</sup>, corresponding to the bending vibration and out-of-plane bending vibration of -CH<sub>3</sub>,<sup>34</sup> and the band at 1060 cm<sup>-1</sup> is attributed to the C-O-C bond stretching vibration.<sup>35</sup> While in the spectrum of PLA-g-PAA, two new peaks at 1706 and 922 cm<sup>-1</sup> appears, corresponding to the C=O and -OH in the carboxyl group of acrylic acid grafted on the surface of PLA

films.<sup>36</sup> These two bands are enhanced with the increase of GY. These results indicate that PAA chains are successfully grafted onto the surface of PLA films.

**2.1.2. Characterization of PLA-g-PAA-Ag.** To explore the effect of AgNO<sub>3</sub> concentration on the amount of AgNPs loaded on the surface of PLA-g-PAA films, PLA-g-PAA-Ag samples prepared at different AgNO<sub>3</sub> concentrations are analyzed by ICP (Figure 2). When the concentration of

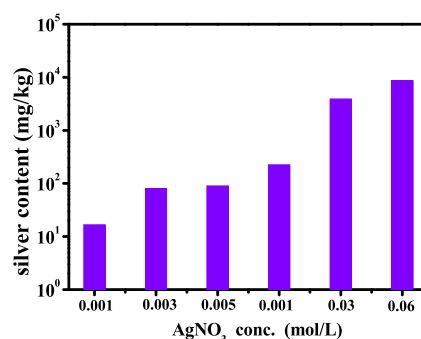


**Figure 2.** Effect of AgNO<sub>3</sub> concentration on the silver content in the samples.

AgNO<sub>3</sub> is 0.001 mol L<sup>-1</sup>, the silver content on the surface of the sample is 1.6 × 10<sup>1</sup> mg/kg. When the concentration increases to 0.06 mol L<sup>-1</sup>, the silver content of PLA-g-PAA-Ag-4 is up to 8.7 × 10<sup>3</sup> mg/kg. The silver loading is positively correlated with the AgNO<sub>3</sub> concentration.

SEM/EDX analyses were also used to characterize the morphology of PLA, PLA-g-PAA-2, and PLA-g-PAA-Ag-4 (Figure 3). It is observed that the surface of the PLA film is smooth with no wrinkles. For the PLA-g-PAA-2 film, a small amount of agglomeration can be observed and the distribution is relatively uniform, which is attributed to the grafted PAA on the surface of the PLA film. Besides agglomeration, a small number of bright spots can be seen on the surface of PLA-g-PAA-Ag-4, corresponding to AgNPs. Figure 3d–f shows the EDX images of PLA-g-PAA-Ag-4. It can be seen that AgNPs are evenly distributed on the surface of PLA even with the highest content. In addition, compared with PLA-g-PAA-2, PLA-g-PAA-Ag-4 shows a more uniform distribution of PAA. It is speculated that the addition of AgNPs may prevent the agglomeration of PAA chains.

To uncover the interaction mechanism between PAA and AgNPs, XPS is used (Figure 4). For PLA-g-PAA-Ag-4, strong peaks at 368.1 and 374.1 eV (Figure 4A) are observed, corresponding to the Ag 3d<sub>5/2</sub> and Ag 3d<sub>3/2</sub> binding

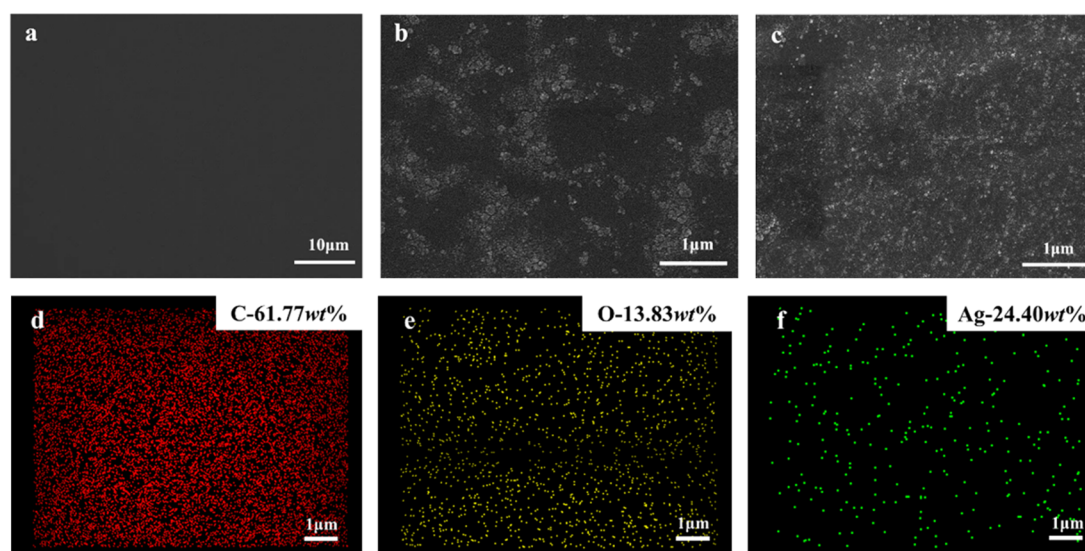


**Figure 3.** SEM images of (a) PLA, (b) PLA-g-PAA-2, and (c) PLA-g-PAA-Ag-4 and (d–f) EDX images of main elemental distribution of PLA-g-PAA-Ag-4.

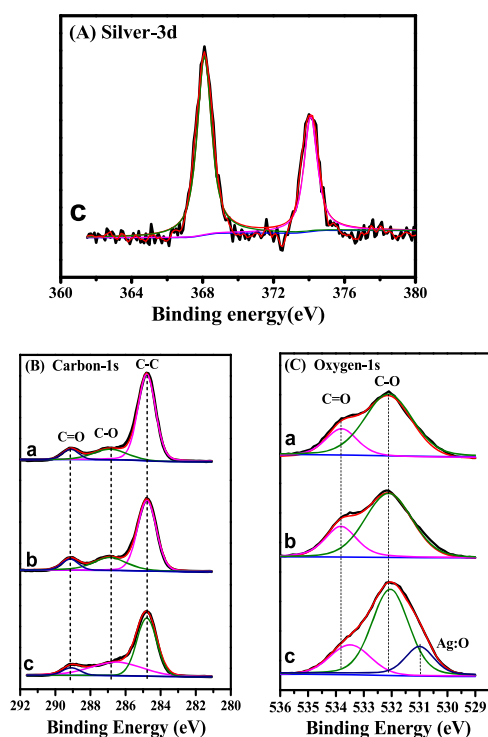


**Figure 4.** Elemental XPS-spectra of (A) Ag 3d, (B) C 1s, and (C) O 1s; (a) PLA film, (b) PLA-g-PAA-2 film, and (c) PLA-g-PAA-Ag-4 film.

energies, respectively.<sup>37</sup> These results also confirm that Ag is loaded on the surface of PLA-g-PAA-Ag-4. As shown in Figure 4B, C 1s signals of PLA films can be resolved into three peaks at 284.8, 286.9, and 289.1 eV, which correspond to C–C, C–O, and C=O functional groups on PLA films, respectively.<sup>38</sup> For PLA-g-PAA-2 and PLA-g-PAA-Ag-4, there are no changes in the C 1s peaks, which implies that carbon atoms do not directly interact with Ag atoms. The O 1s spectrum of PLA (Figure 4C) exhibits two peaks centered at 533.8 and 532.1 eV, which are assigned to the C=O and C–O groups, respectively. For PLA-g-PAA-2, no obvious changes can be

observed in the O 1s spectrum, which indicates that the grafted PAA on the surface of PLA has little effect on the chemical environment of the O atom. However, for PLA-g-PAA-Ag-4, a new peak at 531.0 eV appears corresponding to Ag:O, which suggests the interaction between the oxygen atoms and Ag atoms (Table 1). Similar results have been reported in the

**Table 1.** Assignments of Binding Energies of Main XPS Regions

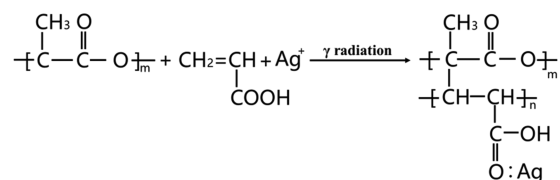
element	binding energy (eV)			assignment
	PLA	PLA-g-PAA-2	PLA-g-PAA-Ag-4	
C 1s 1	284.8	284.8	284.8	aliphatic CH
C 1s 2	286.9	286.8	286.8	C–O
C 1s 3	289.1	289.1	289.1	C=O
O 1s 1	533.8	533.8	533.4	C=O
O 1s 2	532.1	532.1	532.1	C–O
O 1s 3			531.0	Ag:O
Ag 3d 1			368.1	Ag <sup>0</sup>
Ag 3d 2			374.1	Ag <sup>0</sup>

literature.<sup>39</sup> Furthermore, the binding energy of C=O shifts from 533.8 to 533.4 eV, indicating that the coordination bonds are formed between Ag and oxygen atoms in carbon–oxygen double bonds and the electron clouds are migrated. The possible interaction between AgNPs and PAA is depicted in Scheme 1.

## 2.2. Hydrophilicity and Antibacterial Properties of Radiation-modified PLA Films.

The water contact angle is used to evaluate the surface hydrophilicity of PLA films, as

**Scheme 1.** Diagram of the Interaction between AgNPs and PAA



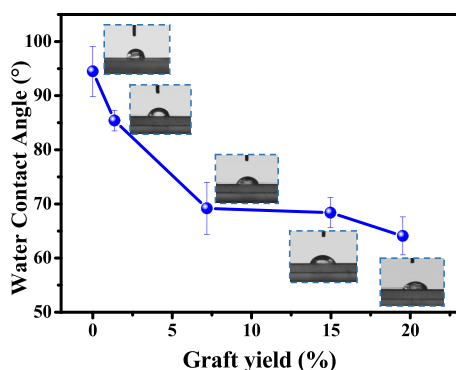


Figure 5. Water contact angles of PLA and PLA-g-PAA.

Table 2. Water Contact Angle of PLA-g-PAA-Ag with Different Ag Content

sample	Ag content (mg/kg)	contact angle (°)
PLA-g-PAA-2	0	69.8
PLA-g-PAA-Ag-1	$1.6 \times 10^1$	68.4
PLA-g-PAA-Ag-2	$8.0 \times 10^1$	71.0
PLA-g-PAA-Ag-3	$9.0 \times 10^1$	71.7
PLA-g-PAA-Ag-4	$2.2 \times 10^2$	74.2
PLA-g-PAA-Ag-5	$3.9 \times 10^3$	75.3
PLA-g-PAA-Ag-6	$8.7 \times 10^3$	81.1

shown in Figure 5, Tables 2 and 3. As expected, the water contact angle of the PLA-g-PAA film decreases with the increase of GY. For example, the water contact angle of the pure PLA film was  $94.5^\circ$ , which decreased to  $64.1^\circ$  with the increase of GY to 19.53%. Compared with PLA-g-PAA-2, the contact angle of PLA-g-PAA-Ag increased with the increase of AgNP content, which is due to the poor hydrophilicity of AgNPs on the surface.<sup>40</sup> However, the contact angle of PLA-g-PAA-Ag-1 prepared with lower  $\text{AgNO}_3$  concentration did not show an obvious increase as compared to PLA-g-PAA-2 with the same monomer concentration.

The antibacterial activities of the PLA films against *E. coli* and *S. aureus* were studied on solid growth media, and the results are shown in Table 3. All of the obtained PLA-g-PAA-Ag films exhibit higher antibacterial activity than that of the neat PLA film while the PLA-g-PAA-2 film doesn't show improved antibacterial activity. Meanwhile, the antibacterial effects of the modified films are increased with the increase of AgNPs content. When the silver content reaches  $1.6 \times 10^1$

mg/kg, the antibacterial rate against *S. aureus* is 84%, and when the content reaches  $9.0 \times 10^1$  mg/kg, the antibacterial rate of the sample against the two species of bacteria are both higher than 99%. Furthermore, the PLA-g-PAA-Ag show higher antibacterial activity against *E. coli* than *S. aureus*, which is due to the antibacterial mechanisms of AgNPs and the different structure of bacteria. The contact reaction between AgNPs and cells occurs when AgNPs penetrate the cell wall, which leads to the destruction or dysfunction of the inherent components of bacteria and the death of bacteria. AgNPs is more difficult to penetrate the cell wall of *S. aureus* composed of a thick layer of peptidoglycan, which result in a lower antibacterial activity compared to *E. coli*.<sup>22,41</sup>

**2.3. Thermal Stability of Radiation-modified PLA Films.** The TGA results of PLA, PLA-g-PAA-2, and PLA-g-PAA-Ag-4 films are shown in Figure 6. The temperature of 5% weight loss ( $T_{5\%}$ ) and the maximum degradation temperature ( $T_{\max}$ ) of neat PLA films were 332 and  $365.3^\circ\text{C}$ , respectively. While the  $T_{5\%}$  and  $T_{\max}$  of the PLA-g-PAA-2 film decreased to 313.7 and  $354.0^\circ\text{C}$  (a decrease of nearly  $10^\circ\text{C}$ ), respectively. This is attributed to the poor thermal stability of PAA. The  $T_{5\%}$  of PLA-g-PAA-Ag-4 is  $312.4^\circ\text{C}$ , which is similar to that of the PLA-g-PAA-2 film. However,  $T_{\max}$  is  $363.2^\circ\text{C}$ , which is close to that of the neat PLA film. It is suggested that the loaded AgNPs can improve the thermal stability of the PLA matrix of the PLA-g-PAA film.<sup>42,43</sup>

### 3. CONCLUSIONS

PLA films with improved hydrophilicity and antimicrobial properties were prepared by  $\gamma$ -ray radiation-induced simultaneous grafting polymerization and Ag reduction. The degree of grafting increased with the increase of AAC monomer concentration. The maximum GY reached 19.53% at 4.82 mol/L AAC concentration, and the water contact angle of PLA films decreased from  $94.5^\circ$  (neat PLA film) to  $64.1^\circ$ . The PLA film loaded with AgNPs, which showed hydrophilic and antimicrobial capabilities, was successfully prepared. The AgNPs were loaded onto the surface of PLA films via grafted PAA chains, which endowed the films with excellent hydrophilicity and antibacterial properties. The antibacterial rate of the grafted film (PLA-g-PAA-Ag-3) to *E. coli* and *S. aureus* were more than 99%, while maintaining the hydrophilicity. This work opens up an environment-friendly approach to prepare PLA films with excellent antibacterial and hydrophilic properties.

Table 3. Antibacterial Activity of PLA Films against *E. coli* and *S. aureus*

samples	<i>E. coli</i>		<i>S. aureus</i>	
	log reduction (R)	antibacterial rate (%)	log reduction (R)	antibacterial rate (%)
contrast sample (PE)				
PLA films	0.17	32	0.55	72
PLA-g-PAA-2	0.21	38	0.43	63
PLA-g-PAA-Ag-1	4.0	>99	0.8	84
PLA-g-PAA-Ag-2	>5.5	>99	2.3	99
PLA-g-PAA-Ag-3	>5.5	>99	3.1	>99
PLA-g-PAA-Ag-4	>6.3	>99	>4.6	>99
PLA-g-PAA-Ag-5	>6.3	>99	>4.6	>99
PLA-g-PAA-Ag-6	>6.3	>99	4.6	>99

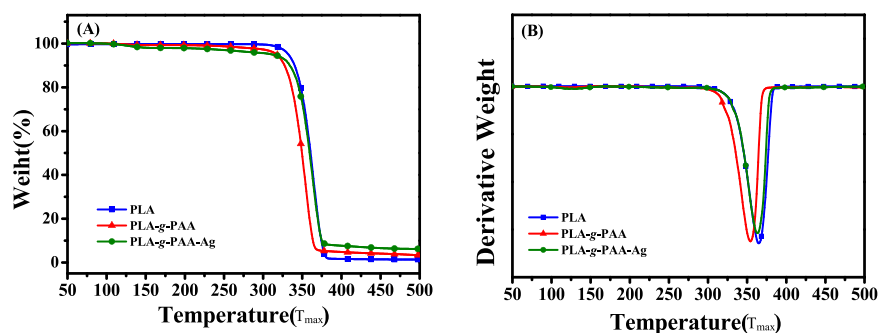


Figure 6. (A) TGA and (B) DTG curves of PLA, PLA-g-PAA-2, and PLA-g-PAA-Ag-4.

## 4. EXPERIMENTAL SECTION

**4.1. Materials.** PLA (optical purity > 99%,  $M_n = 47$  kg/mol,  $DPI = 2.61$ ) was supplied by Zhejiang Haizheng Biomaterials Co., Ltd. Silver nitrate ( $AgNO_3$ ) was obtained from Beijing TongGuang Fine Chemicals Company. The acrylic acid (AAc) monomer was obtained from Tianjin Fuchen Reagent Factory. Absolute ethanol was purchased from Beijing Chemical Factory. All reagents and solvents were analytical-grade chemicals and were used directly without further purification.

**4.2. Fabrication of Modified PLA Films.** PLA pellets were dried at 80 °C under vacuum for 12 h to remove the residual  $H_2O$  in PLA. PLA films were obtained by melt pressing for 5 min in 190 °C and then cut into small pieces with a size of  $6.5 \times 2.5$  cm<sup>2</sup>.

A series of monomer solutions was prepared by adding acrylic acid with different volumes into ethanol/water = 8:2 solvent. PLA films and monomer solution were added into glass tubes, and then the mixture was saturated with nitrogen for 20 min to remove oxygen. Sealed glass tubes were irradiated using a <sup>60</sup>Co source at the Department of Applied Chemistry of Peking University at room temperature. The dose was 10 kGy, and the dose rate was 50 Gy/min. The obtained films were washed three times and soaked in excessive absolute ethanol for 20 h at room temperature to remove residual unreacted monomer and homopolymers of polyacrylic acid (PAA) and then dried in an oven at 60 °C to constant mass. The resulting films were called PLA-g-PAA in short.

A series of grafting solutions with Ag was prepared by adding  $AgNO_3$  with different weights to the solution within AAc (2.41 mol L<sup>-1</sup>). The graft films were treated under the same irradiation and post-treatment conditions. The resulting films were denoted PLA-g-PAA-Ag.

The abbreviations of the samples with different monomer concentrations and  $AgNO_3$  concentrations are listed in Table 4.

**4.3. Characterization.** The grafting yield (GY) was determined gravimetrically using eq 1

$$GY(\%) = \frac{W_1 - W_0}{W_0} \times 100\% \quad (1)$$

where  $W_1$  and  $W_0$  denote the weights of grafted and original PLA films, respectively.

FTIR measurements were carried out using a Bruker Tensor 27 spectrometer within the wavenumber range of 500–4000 cm<sup>-1</sup>. A total of 32 scans/sample were taken, with a resolution of 4 cm<sup>-1</sup>. The surface morphology of PLA films was observed

Table 4. Conditions of Grafted PLA Samples

sample name	monomer concentration of AAc (mol L <sup>-1</sup> )	concentration of $AgNO_3$ (mol L <sup>-1</sup> )
PLA		
PLA-g-PAA-1	1.31	
PLA-g-PAA-2	2.41	
PLA-g-PAA-3	3.61	
PLA-g-PAA-4	4.82	
PLA-g-PAA-Ag-1	2.41	0.001
PLA-g-PAA-Ag-2	2.41	0.003
PLA-g-PAA-Ag-3	2.41	0.005
PLA-g-PAA-Ag-4	2.41	0.01
PLA-g-PAA-Ag-5	2.41	0.03
PLA-g-PAA-Ag-6	2.41	0.06

by a SEM (JEOL JSM-7500F, Japan) and an energy-dispersive X-ray spectrometer (OXFORD INCAx-sight). The sample was coated with platinum before observation. The instrument was operated at an accelerating voltage of 5 kV and 10  $\mu$ A. The chemical composition of the surface of PLA films was semiquantitatively examined by X-ray photoelectron spectrometry (Kratos AXIS Supra). Thermogravimetric analysis (TGA) of the samples was carried out with a TGA Q-500 series analyzer (TA Instruments) with a temperature range of 35–500 °C. The heating rate was 10 K/min with a continuous flow of nitrogen at 50 mL/min.

To determine the surface properties of samples, the water contact angles were measured on an OCA 20 contact-angle system (Dataphysics, Stuttgart, Germany) at 25 °C. The average contact angle values were calculated by measuring at least five different positions of each film. The antibacterial activities of the PLA films against *E. coli* and *S. aureus* were evaluated according to the standard procedure (ISO22196-2011).

## AUTHOR INFORMATION

### Corresponding Author

\*E-mail: clyzxq@bift.edu.cn.

### ORCID

Rui Wang: 0000-0001-5886-3261

Xiu-Qin Zhang: 0000-0002-8687-4280

### Notes

The authors declare no competing financial interest.

## ACKNOWLEDGMENTS

The National Natural Science Foundation of China (Grant No. 51673003) and the Beijing Great Wall Scholars Incubator Program (No. CTT&TCD20180321) are acknowledged.

## REFERENCES

- (1) Wang, D. Y.; Gohs, U.; Kang, N. J.; Leuteritz, A.; Boldt, R.; Wagenknecht, U.; Heinrich, G. Method for Simultaneously improving the thermal stability and mechanical properties of poly(lactic acid): effect of high-energy electrons on the morphological, mechanical, and thermal properties of PLA/MMT nanocomposites. *Langmuir* **2012**, *28*, 12601–12608.
- (2) Urayama, H.; Kanamori, T.; Kimura, Y. Properties and Biodegradability of Polymer Blends of Poly(L-lactide)s with Different Optical Purity of the Lactate Units. *Macromol. Mater. Eng.* **2002**, *287*, 116–121.
- (3) Lim, L. T.; Auras, R.; Rubino, M. Processing technologies for poly(lactic acid). *Prog. Polym. Sci.* **2008**, *33*, 820–852.
- (4) Li, X. L.; Wang, R.; Yang, C.; Dong, Z.; Zhang, X. Q.; Wang, D. Y. Effect of Poly(D-lactic acid) Block Copolymers with Soft Chains on the Tensile Behavior of Poly(L-lactic acid). *Chin. J. Polym. Sci.* **2018**, *5*, 598–606.
- (5) Li, X. L.; Zhang, X.; Liu, G.; Yang, Z.; Yang, B.; Qi, Y.; Wang, R.; Wang, D. Y. Effect of stereocomplex crystal and flexible segments on the crystallization and tensile behavior of poly(l-lactide). *RSC Adv.* **2018**, *8*, 28453–28460.
- (6) Chu, C. C. Materials for absorbable and nonabsorbable surgical sutures. *Woodhead Publ. Ser. Text.* **2013**, 275–334.
- (7) Serra, T.; Ortiz-Hernandez, M.; Engel, E.; Planell, J. A.; Navarro, M. Relevance of PEG in PLA-based blends for tissue engineering 3D-printed scaffolds. *Mater. Sci. Eng., C* **2014**, *38*, 55–62.
- (8) Kao, C. T.; Lin, C. C.; Chen, Y. W.; Yeh, C. H.; Fang, H. Y.; Shie, M. Y. Poly(dopamine) coating of 3D printed poly(lactic acid) scaffolds for bone tissue engineering. *Mater. Sci. Eng., C* **2015**, *56*, 165–173.
- (9) Novikova, L. N.; Novikov, L. N.; Kellerth, J. O. Biopolymers and biodegradable smart implants for tissue regeneration after spinal cord injury. *Curr. Opin. Neurol.* **2003**, *16*, 711–715.
- (10) Mhlanga, N.; Sinha Ray, S.; Lemmer, Y.; Wesley-Smith, J. Polylactide-based Magnetic Spheres as Efficient Carriers for Anticancer Drug Delivery. *ACS Appl Mater Interfaces.* **2015**, *7*, 22692–22701.
- (11) Yang, B.; Wang, R.; Ma, H. L.; Li, X.; Brunig, H.; Dong, Z.; Qi, Y.; Zhang, X. Q. Structure Mediation and Properties of Poly(l-lactide)/Poly(d-lactide) Blend Fibers. *Polymers* **2018**, *10*, No. 1353.
- (12) Lee, S. H.; Yeo, S. Y. Improvement of hydrophilicity of polylactic acid (PLA) fabrics by means of a proteolytic enzyme from *Bacillus licheniformis*. *Fibers Polym.* **2016**, *17*, 1154–1161.
- (13) Zuo, Y.; Gu, J.; Yang, L.; Qiao, Z.; Tan, H.; Zhang, Y. Preparation and characterization of dry method esterified starch/polylactic acid composite materials. *Int. J. Biol. Macromol.* **2014**, *64*, 174–180.
- (14) Yin, J. B.; Lu, X. C.; Yan, L. C.; et al. Preparation and Characterization of Plasticized Poly(Lactic acid) Citrate Esters as Plasticizers. *Gaofenzi Cailiao Kexue Yu Gongcheng* **2008**, *24*, 151–154.
- (15) Zhang, D. S.; Wang, Z. Y. Structural Design and Product Development of Moisture-absorbent & Sweat-exhausting Polyester Fiber. *Fangzhi Daobao.* **2018**, *5*, 55–59.
- (16) González, E.; Shepherd, L. M.; Saunders, L.; Frey, M. W. Surface Functional Poly(lactic acid) Electrospun Nanofibers for Biosensor Applications. *Materials* **2016**, *9*, 47.
- (17) Wang, N.; Zang, Y. J.; Ren, G. Z.; Wu, Q. L. Fabrication and Properties of Porous Scaffolds of PLA-PEG Biocomposite for Bone Tissue Engineering. *Mater. Sci. Forum* **2014**, *789*, 130–135.
- (18) Yue, Z.; You, Z.; Yang, Q.; Lv, P.; Yue, H.; Wang, B.; Ni, D.; Su, Z.; Wei, W.; Ma, G. Molecular structure matters: PEG-b-PLA nanoparticles with hydrophilicity and deformability demonstrate their advantages for high-performance delivery of anti-cancer drugs. *J. Mater. Chem. B* **2013**, *1*, 3239–3247.
- (19) Ouyang, P.; Kang, Y. Q.; Yin, G. F.; Huang, Z. B.; Yao, Y. D.; Liao, X. M. Fabrication of hydrophilic paclitaxel-loaded PLA-PEG-PLA microparticles via SEDS process. *Front. Mater. Sci. China* **2009**, *3*, 15–24.
- (20) Wang, Y.; Ren, R.; Ling, J.; Sun, W.; Shen, Z. One-pot “grafting-from” synthesis of amphiphilic bottlebrush block copolymers containing PLA and PVP side chains via tandem ROP and RAFT polymerization. *Polymer* **2018**, *138*, 378–386.
- (21) Petzetakis, N.; Dove, A. P.; O’Reilly, R. K. Cylindrical micelles from the living crystallization-driven self-assembly of poly(lactide)-containing block copolymers. *Chem. Sci.* **2011**, *2*, 955–960.
- (22) Choi, J. B.; Park, J. S.; Khil, M. S.; Gwon, H. J.; Lim, Y. M.; Jeong, S. I.; Shin, Y. M.; Nho, Y. C. Characterization and antimicrobial property of poly(acrylic acid) nanogel containing silver particle prepared by electron beam. *Int. J. Mol. Sci.* **2013**, *14*, 11011–11023.
- (23) Tsou, C. H.; Yao, W. H.; Lu, Y. C.; Chen, J.; Wang, R.; Su, C.; Hung, W. S.; De Guzman, M.; Suen, M. C.; et al. Antibacterial Property and Cytotoxicity of a Poly(lactic acid)/Nanosilver-Doped Multiwall Carbon Nanotube Nanocomposite. *Polymers* **2017**, *9*, No. 100.
- (24) Kara, H. H.; Xiao, F.; Sarker, M.; Jin, T. Z.; Sousa, A. M. M.; Liu, C. K.; Tomasula, P. M.; Liu, L. Antibacterial poly(lactic acid) (PLA) films grafted with electrospun PLA/allyl isothiocyanate fibers for food packaging. *J. Appl. Polym. Sci.* **2015**, *133*, 726–736.
- (25) Wei, J.; Liu, J.; Qiang, J.; Yang, L.; Wan, Y.; Wang, H.; Gao, W.; Ko, F. Antibacterial Performance of Chitin Nanowhisker Reinforced Poly(lactic acid) Composite Nanofiber Membrane. *Adv. Sci. Lett.* **2012**, *10*, 649–651.
- (26) Mao, L.; Jin, Y.; Liu, Y. J.; Bai, Y. K. Preparation and Characterization of Polylactic Acid-Polypyrrole/Silver Multilayer Composite Antibacterial Film. *Biaomian Jishu* **2019**, *48*, 154–160.
- (27) Fei, Y.; Chen, Y.; Wang, H.; Gao, W.; Yang, R.; Wan, Y. Preparation, characterization of antibacterial PLA/TP nanofibers. *Fibers Polym.* **2011**, *12*, 340–344.
- (28) Hidzir, N. M.; Hill, D. J. T.; Martin, D.; Grøndahl, L. Radiation-induced grafting of acrylic acid onto expanded poly-(tetrafluoroethylene) membranes. *Polymer* **2012**, *53*, 6063–6071.
- (29) Luk, J. Z.; Cork, J.; Cooper-White, J.; Grøndahl, L. Use of two-step grafting to fabricate dual-functional films and site-specific functionalized scaffolds. *Langmuir* **2015**, *31*, 1746–1754.
- (30) Liu, M.; Yin, Y.; Fan, Z.; Zheng, X.; Shen, S.; Deng, P.; Zheng, C.; Teng, H.; Zhang, W. The effects of gamma-irradiation on the structure, thermal resistance and mechanical properties of the PLA/EVOH blends. *Nucl. Instrum. Methods Phys. Res., Sect. B* **2012**, *274*, 139–144.
- (31) Chen, H.; Peng, C.; Yao, Y.; Wang, J.; Chen, Z.; Yang, Z.; Xia, L.; Liu, S. Preparation and characterization of poly(L-lactide) membranes prepared by  $\gamma$ -radiation-induced grafting of N-vinyl pyrrolidone. *J. Appl. Polym. Sci.* **2009**, *114*, 3152–3157.
- (32) Ting, T. M.; Nasef, M. M.; Hashim, K. Modification of nylon-6 fibres by radiation-induced graft polymerisation of vinylbenzyl chloride. *Radiat. Phys. Chem.* **2015**, *109*, 54–62.
- (33) Pukhova, I. V.; Savkin, K. P.; Laput, O. A.; Lytkina, D. N.; Botvin, V. V.; Medovnik, A. V.; Kurzina, I. A. Effects of ion- and electron-beam treatment on surface physicochemical properties of polylactic acid. *Appl. Surf. Sci.* **2017**, *422*, 856–862.
- (34) Mishra, S.; Usha Rani, G.; Sen, G. Microwave initiated synthesis and application of polyacrylic acid grafted carboxymethyl cellulose. *Carbohydr. Polym.* **2012**, *87*, 2255–2262.
- (35) Gore, P. M.; Kandasubramanian, B. Heterogeneous wettable cotton based superhydrophobic Janus biofabric engineered with PLA/functionalized-organoclay microfibers for efficient oil–water separation. *J. Mater. Chem. A* **2018**, *6*, 7457–7479.
- (36) Mandal, D. K.; Bhunia, H.; Bajpai, P. K.; Chaudhari, C. V.; Dubey, K. A.; Varshney, L. Radiation-induced grafting of acrylic acid onto polypropylene film and its biodegradability. *Radiat. Phys. Chem.* **2016**, *123*, 37–45.
- (37) Ferraria, A. M.; Boufi, S.; Battaglini, N.; Botelho do Rego, A. M.; ReiVilar, M. Hybrid systems of silver nanoparticles generated on cellulose surfaces. *Langmuir* **2010**, *26*, 1996–2001.
- (38) Liu, H.; Xie, D.; Qian, L.; Deng, X.; Leng, Y. X.; Huang, N. The mechanical properties of the ultrahigh molecular weight polyethylene

(UHMWPE) modified by oxygen plasma. *Surf. Coat. Technol.* **2011**, *205*, 2697–2701.

(39) Wang, J.; Chen, H.; Chen, Z.; Chen, Y.; Guo, D.; Ni, M.; Liu, S.; Peng, C. In-situ formation of silver nanoparticles on poly (lactic acid) film by gamma-radiation induced grafting of N-vinyl pyrrolidone. *Mater. Sci. Eng., C* **2016**, *63*, 142–149.

(40) Ho, J. Y.; Liu, T. Y.; Wei, J. C.; Wang, J. K.; Wang, Y. L.; Lin, J. J. Selective SERS detecting of hydrophobic microorganisms by tricomponent nanohybrids of silver-silicate-platelet-surfactant. *ACS Appl. Mater. Interfaces* **2014**, *6*, 1541–1549.

(41) Shrivastava, S.; Bera, T.; Singh, S.; Singh, G.; Ramachandrarao, P.; Dash, D. Characterization of Antiplatelet Properties of Silver Nanoparticles. *ACS Nano* **2009**, *3*, 1357–1364.

(42) Vukoje, I. D.; Vodnik, V. V.; Džunuzović, J. V.; Džunuzović, E. S.; Marinović-Cincović, M. T.; Jeremić, K.; Nedeljković, J. M. Characterization of silver/polystyrene nanocomposites prepared by in situ bulk radical polymerization. *Mater. Res. Bull.* **2014**, *49*, 434–439.

(43) Rhim, J. W.; Wang, L. F.; Lee, Y.; Hong, S. I. Preparation and characterization of bio-nanocomposite films of agar and silver nanoparticles: laser ablation method. *Carbohydr. Polym.* **2014**, *103*, 456–465.